The Journal of the Acoustical Society of America

DECEMBER 08 2004

Measurement of in-duct acoustic properties by using a single microphone with fixed position

Y. S. Choy; Lixi Huang

J. Acoust. Soc. Am. 116, 3498–3504 (2004)
https://doi.org/10.1121/1.1811476

Measurement of in-duct acoustic properties by using a single microphone with fixed position

Y. S. Choy and Lixi Huang[a)]
Department of Mechanical Engineering, The Hong Kong Polytechnic University, Hunghom, Kowloon, Hong Kong

(Received 13 April 2004; revised 12 August 2004; accepted 10 September 2004)

Acoustic properties of sound absorption materials and other acoustic structures can be measured in an impedance tube using the well-established two-microphone method to resolve the two traveling wave components of a standing wave pattern. The accuracy of such measurements depends crucially on the calibration of the two microphones placed in close proximity. To eliminate such calibration, the one-microphone method [Chu, J. Acoust. Soc. Am. **80**, 555–560 (1986)] uses the same microphone to probe at two positions sequentially using the voltage driving the loudspeaker as a reference signal. A variant of this method is introduced in this study in which the microphone is fixed at one position while a rigid end plate moves between two positions to resolve the standing wave. The sound source is installed as a side branch, and its driving signal is also used as a reference in the two-step measurement. Close agreement is found with the established two-microphone method, and factors which might affect the accuracy of the new technique are discussed. As a demonstration of the robustness of the method, a low-budget electret microphone is used and the result also matches well with those obtained by the two-microphone method with high-quality condenser type microphones. [DOI: 10.1121/1.1811476]

PACS numbers: 43.55.Ev, 43.85.Bh [DKW] Pages: 3498–3504

I. INTRODUCTION

There are four methods to determine the in-duct acoustic properties, such as the reflection coefficient and absorption coefficient. They are the standing wave method using a probe microphone, multi-point, two-microphone, and one-microphone methods. Their strengths and weaknesses have been discussed by Jones and Parrott (1989).

The so-called standing wave method (SWR) (Lippert, 1953) uses a probe microphone to measure the ratio of the successive maxima and minima of a standing wave pattern in order to find out the acoustic impedance, from which the reflection and absorption coefficients are deduced. This is a tedious and time-consuming process. The multi-point method uses one microphone to take measurements at multiple points, and the least-square method is used to curve-fit the measured pattern and deduce the acoustic properties. Two to six pressure measurements per half-wavelength are required (Jones and Parrott, 1989). Again, the measurement points can be varied by using a traversing probe microphone. The main weakness of both SWR and multi-point methods is the requirement of the hardware movement of microphone, which is time consuming. To overcome this problem, the two-microphone method was introduced by Seybert and Ross (1977). Two microphones are placed at two different positions with a certain separation distance. The signals from the two microphones are acquired at the same time in order to find out the transfer function between them, from which the forward and backward waves in a standing wave pattern are resolved. Random excitation is used to find out the auto-spectral and cross-spectral densities of the two locations so that the whole spectrum of acoustic properties can be found at once. This method was further developed by Chung and Blaser analytically and experimentally (1980a, b). Their method involved the decomposition of the waveform into the incident and reflected components using a simple transfer function of the pressures at two locations. The excitation signal can be random or harmonic. The comparison between the transfer function method and SWR with different selected points was investigated in detail by Chu (1988). The absorption and impedance found by the two-microphone method with varied microphone separation distance is better than those with fixed separation and SWR method. A similar approach for different distances between two measurement points was also taken by Fahy (1984). Chu (1986a) also extended the transfer function studies by adding the effect of tube attenuation.

Compared with the SWR and multiple-point methods, the two-microphone method saves time but requires the knowledge of accurate amplitude and phase relationships between the two microphones, so the calibration is necessary before taking a measurement. The calibration is carried out by swapping the pair of microphones which are flush mounted on the duct with absorptive termination according to ISO 10534-2 (1998). To eliminate the calibration, Chu (1986b) introduced the so-called one-microphone method in which a single microphone is used to measure sound at the two measurement points of an otherwise two-microphone rig. In this sense, the methodology is similar to the two-microphone method. Signals taken from the single microphone at different positions are referenced to the analog signal which drives the loudspeaker. The result is good compared with the SWR method although there are some

[a)]Author to whom correspondence should be addressed. Electronic mail: mmlhuang@polyu.edu.hk

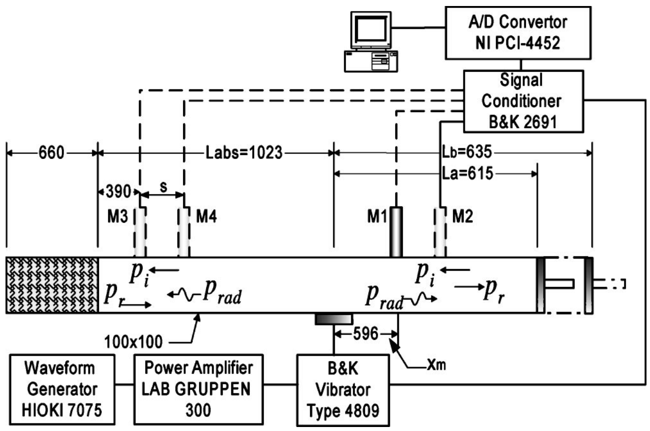

FIG. 1. Experimental setup for the new one-microphone method with provision for the two-microphone method employed for validation purpose.

deviations at low frequencies (<200 Hz). The one-microphone method can eliminate the error of phase mismatch between two microphones. In both two- and one-microphone methods, the two measurements become one when the separation distance between the two measurement positions is equal to an integer multiple of the half-wavelength. In other words, there are frequency blind spots in these methods. To overcome this problem, a third measurement position might be needed. In this study, an alternative configuration for the single microphone method is introduced. In the new design, the loudspeaker is flush mounted to the duct wall as a side branch, and only one fixed microphone insertion hole is provided. A rigid end plate provides the rigid wall boundary and the design is such that the position of the plate can be adjusted easily without the provision of any extra microphone insertion hole. Measurements taken with two positions for the rigid end plate resolve the two traveling wave components. As is shown below, the present one-microphone method is based on an acoustic arrangement different from all previous impedance tube rigs, and the new rig is also expected to bring some convenience in terms of implementation. In what follows, expressions are derived for the reflection and absorption coefficients of the acoustic specimen as a function of the readings of the two-step measurement. Experimental validation is carried out by the two-microphone method. Factors affecting the accuracy of the new single microphone method are discussed towards the end.

II. THEORY

The theoretical model is shown in Fig. 1, which also serves as an illustration of the experimental rig to be described in the next section. The geometry resembles a standard impedance tube. The specimen to be tested is put at one end of the tube at a distance L_{abs} from the center of the flush mounted piston $(x=0)$ driven by a vibrator. A movable rigid plate is installed on the right-hand side at $x=L_a$, L_b during two measurements, respectively. The measurement microphone (labeled M1) is located at $x=x_m$, while three other microphones illustrated by broken lines indicate the use of three extra microphones for the validation purpose in this study.

The acoustic field in the duct can be described by the superposition of acoustic radiation from the piston, indicated by p_{rad}, and the standing wave pattern formed by the reflecting ends of the duct, labeled as p_i and p_r for the left- and right-traveling components, respectively. Note that a near field exists around the piston before the radiated waves evolve into plane waves when the frequency is below the cut-on frequency of the duct. In what follows, p_{rad} denotes the complex amplitude of the plane traveling wave and the near field is ignored in the following derivation where measurement points are sufficiently far away from the piston center. Note also that p_i and p_r are the constant amplitudes for the traveling waves throughout the duct length. The pressure at $x=x_m$ (microphone 1) is written as follows:

$$p_1=(p_{rad}+p_r)e^{-ikx_m}+p_ie^{ikx_m}. \tag{1}$$

Note that the time dependence of $\exp(i\omega t)$ is left out of all formulations, and all pressure amplitudes are divided by the complex amplitude of the voltage signal which drives the vibrator–piston assembly. In other words, the pressures measured can be regarded as a result of vibration of a unit amplitude for all measurements.

The normal particle velocity vanishes at the acoustically rigid plate at $x=L_a$, so the relationship between the wave components is

$$p_i=(p_{rad}+p_r)e^{-2ikL_a} \quad \text{or} \quad p_r=p_ie^{2ikL_a}-p_{rad}. \tag{2}$$

Combining Eqs. (1) and (2),

$$p_i=\frac{p_1}{e^{ikx_m}+e^{ik(2L_a-x_m)}}. \tag{3}$$

When the rigid plate is moved to $x=L_b$, the wave components p_i and p_r are changed but the radiation pressure p_{rad} remains unchanged and independent of the reflections at the tube ends. It is implicitly assumed here that the change in the input mechanical impedance from the air in the duct on the piston is negligible when the rigid end plate moves from one position to the next during the two-step measurement. This assumption is validated in the experiment, and the small variation of piston response is analyzed in the next section. The reflection wave components for the rigid end plate position at $x=L_b$ are denoted by p_i' and p_r'. Similar to Eq. (3),

$$p_i'=\frac{p_1'}{e^{ikx_m}+e^{ik(2L_b-x_m)}}. \tag{4}$$

In addition to these equations, the impedance and reflection coefficient at the interface of the absorption material at $x=-L_{abs}$ is assumed to be the same for the two measurements. The reflection coefficient is written as

$$\frac{R}{I}=\frac{p_r}{p_{rad}+p_i}e^{2ikL_{abs}}=\frac{p_r'}{p_{rad}+p_i'}e^{2ikL_{abs}}, \tag{5}$$

where I is the complex amplitude of the total traveling wave incident on the specimen, and R is the complex amplitude of the reflected wave, cf. Fig. 1.

Solving these two equations for p_{rad} and R/I,

$$\frac{R}{I}=\left(\frac{p_r-p_r'}{p_i-p_i'}\right)e^{2ikL_{abs}}. \tag{6}$$

Within Eq. (6), p_i and p_i' can be found from Eqs. (3) and (4), while p_r and p_r' are found from the second equation in (2) when the rigid plate is placed at $x=L_a$ and $x=L_b$, respectively. Hence,

$$p_r-p_r'=p_i e^{2ikL_a}-p_i' e^{2ikL_b}.$$

Substitution of these results into Eq. (6) gives the complex reflection coefficient R/I as well as the energy coefficients of reflection (β) and absorption (α) defined as follows:

$$\frac{R}{I}=\frac{(p_1/p_1')\cos[k(L_b-x_m)]e^{2ikL_a}-e^{ik(L_a+L_b)}\cos[k(L_a-x_m)]}{(p_1/p_1')\cos[k(L_b-x_m)]-e^{ik(L_a-L_b)}\cos[k(L_a-x_m)]}e^{2ikL_{abs}}, \quad \beta=\left|\frac{R}{I}\right|^2, \quad \alpha=1-\beta. \tag{7}$$

When the distance between the measurement microphone and the rigid end plate is a quarter wavelength, say for the second measurement, $k(L_b-x_m)=\pi/2$, the pressure at the measuring point vanishes, $p_1'=0$, and Eq. (7) becomes the type of 0/0. This is similar to what happens in the two-microphone measurement when the distance between the two microphones is a multiple of a half-wavelength. Theoretically, the problem can be resolved by taking the ratio of the derivative with respect to k for $\cos[k(L_b-x_m)]/p_1' \rightarrow -1/(\partial p_1'/\partial k)$, which requires the use of data for the current as well as the neighboring frequencies. Having said that, one must be aware that such a derivative may not be numerically reliable in an experiment where broadband excitation is used, leading to small ripples in the measured data. If, however, harmonic excitation is used, one can always skip this particular frequency during the test. If the result at the particular frequency is definitely desired, one can always move the rigid end plate to a slightly different position. Such a move would be easier to implement in the current device than drilling another microphone insertion hole in the two-microphone method. In the present experimental study, this singularity is not encountered as the operational frequency is chosen to be below 1000 Hz while the quarter-wavelength frequency for $L_b-x_m=40$ mm is 2144 Hz.

III. EXPERIMENTAL VALIDATION

Figure 1 also shows the schema for the experimental rig with lengths labeled in mm. The duct cross section was 100 $\times$100 mm^2. The duct wall was made of 15-mm-thick acrylic, which is believed to be acoustically rigid. The first cut-on frequency of the duct was 1700 Hz. For the purpose of cross-checking, two pairs of B&K $\frac{1}{2}$-in. condenser-type microphones (type number 4189) were installed flush with the duct walls. Microphone 1 (M1) was regarded as the measurement microphone in the present one-microphone method. The additional microphone (M2) was used to couple with M1 to conduct the two-microphone measurement for the reflection coefficient at the surface of the movable rigid plate. Two more microphones (M3,M4) were installed at the left-hand side to measure the acoustic properties of the specimen at $x=-L_{abs}$ for comparison with the results of the one-microphone method. Note that only one microphone, M1, is needed when the device is used in practice. A wide separation distance of 80 mm was used for the microphone pairs in order to have a good measurement accuracy at lower frequencies. The distance between the rigid plate and M1 was 20 mm in the first measurement and 40 mm in the second measurement when the rigid plate was moved by $L_b-L_a=20$ mm. The movement was increased to 40 mm for frequencies lower than 200 Hz. The movable plate was tightened after the adjustment of its location. The microphones were supported by B&K's Nexus four-channel conditioning amplifier (type 2691), and the signals were acquired through the National Instruments' AD conversion card type PCI-4452. The voltage signal fed to the vibrator (B&K type 4809), which drove the flush-mounted piston, was also captured together with the microphone signals. A harmonic analog signal was generated by a function generator (Hioki 7050), amplified by B&K's power amplifier (LAB Gruppen 300) before it was fed to the vibrator. The frequencies ranged from 100 to 1000 Hz with an interval of 20 Hz. The advantage of the pure tone tests is its better signal-to-noise ratio than broadband excitation, which is good for the comparison between the two-microphone method and the present method. The piston had a surface area of 50$\times$50 mm^2, flush mounted in the middle of the duct. In order to allow free oscillation of the piston, there was a 2-mm gap between the edges of the duct and the piston. To avoid noise leaking through the gap, a 0.6-mm-thick flexible rubber was used to seal the gap. Fiberglass of density 40 kg/m^3 and flow resistivity of about 9000 kg/m^{3}s were used as the acoustic specimen to be tested in the left-hand side tube. Tests were conducted with the test section filled up by fiberglass to three different depths: 60, 185, and 660 mm. Since the duct was not very short, the acoustic attenuation had to be taken into account when deducing the reflection coefficient. This is discussed in Sec. IV.

Figure 2 shows the comparison of the absorption coefficient α of the glass fiber measured by the present one-microphone method (open circles) and the two-microphone

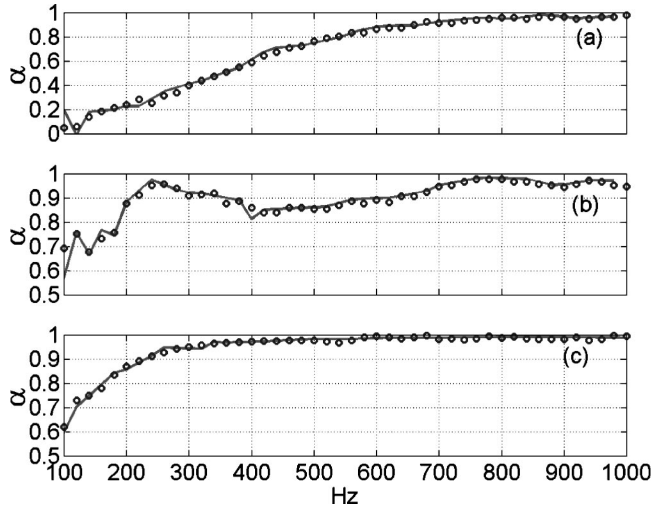

FIG. 2. Comparison of the absorption coefficient between the present method (○) and the two-microphone method (———). (a) is for the absorption material of 60 mm in depth, (b) 185 mm, and (c) 660 mm.

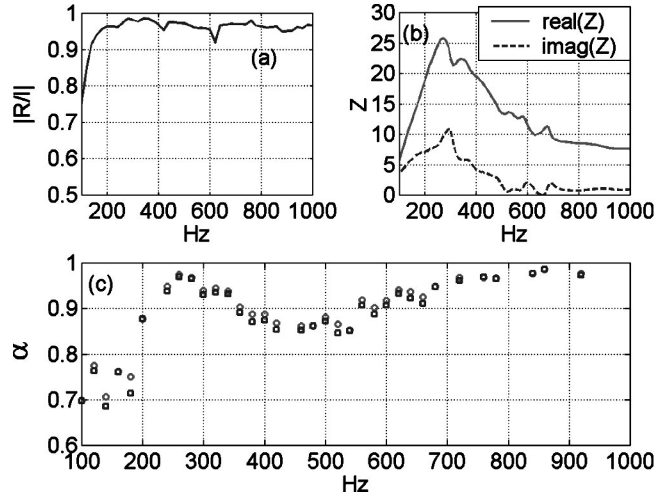

FIG. 3. Effect of the rigidity of the movable plate. (a) is the reflection coefficient at the surface of the movable plate measured by the two-microphone method. (b) is the real (———) and imaginary (– –) parts of the normalized impedance at the surface of the movable plate. (c) is the comparison of the absorption coefficient calculated by Eq. (7) (○) and Eq. (8) (□).

method (solid line). Figures 2(a)–(c) are the results for the fiberglass filling of depth 60, 85, and 660 mm, respectively. The agreement between the two methods for all three tests is good except a few points below about 150 Hz. Above 150 Hz, the mean deviations between the two methods are 1.4%, 1.1%, and 0.6% for the three tests, respectively. Similar results can be obtained by using random signal excitation to the piston.

IV. MEASUREMENT ACCURACY

This section is devoted to the investigation of the effects of various special factors which might affect the accuracy of the current measurement technique. These factors include the vibration of the so-called rigid plate, the effect of the end plate position on the piston response, noise leaking in the piston gap, and other noise attenuation mechanisms present in the system. The attenuation would be significant if the distance between the measurement microphone M1 and the acoustic specimen is very large. For the errors caused by the finite size of the microphone sensing membrane, calibration error of phase mismatch between two microphones, spectral analysis for signals with noisy environment, etc., the readers are referred to the earlier works of Seybert and Soenarko (1981) as well as Bodén and Åborn (1986).

A. Rigidity of the movable plate

If the rigid plate is not entirely rigid, sound reflection on its surface would be less than 100%. The extent to which the rigid plate assumption was correct for the current rig was assessed by the reflection coefficient by the two-microphone method using microphones M3 and M4 shown in Fig. 1. The ratio of linear amplitudes, $|R/I|$, is shown in Fig. 3(a). On average, $|R/I|$ was about 0.96. However, below 100 Hz, it could be lower than 0.9. The impedance of the so-called rigid plate is normalized by that of air, $Z=p'/(\rho_0 c_0 u)$, and the result is shown in Fig. 3(b). When the finite impedance is used for the end plate, the absorption coefficient for the acoustic specimen is recalculated as

$$\alpha=1-\left|\left[\frac{Z+1}{Z-1}\right]\frac{\left[\dfrac{p_1}{p_1'}\right]\left[\dfrac{(Z-1)e^{ikx_m}+(Z+1)e^{i(2kL_b-x_m)}}{(Z-1)e^{ikx_m}+(Z+1)e^{i(2kL_a-x_m)}}\right]e^{2ikL_a}-e^{2ikL_b}}{\left[\dfrac{p_1}{p_1'}\right]\left[\dfrac{(Z-1)e^{ikx_m}+(Z+1)e^{i(2kL_b-x_m)}}{(Z-1)e^{ikx_m}+(Z+1)e^{i(2kL_a-x_m)}}\right]-1}\right|^2. \tag{8}$$

Figure 3(c) compares α deduced from the rigid-plate assumption (open circles) and that from the above formula (open squares). It is found that the correction of the end plate vibration amounts to about 1.5% in terms of α except for 180 Hz where a deviation of 4.0% is found. The conclusion is that the end plate vibration is not significant.

B. Effect of sound attenuation in the duct system

A long duct of over 1.6 m is used in the present setup in Fig. 1. This may cause excessive sound attenuation due to the frictional loss, heat transfer, etc. There may also be a certain amount of noise leaking through the clearance between the piston and the duct wall. These losses can be cal-

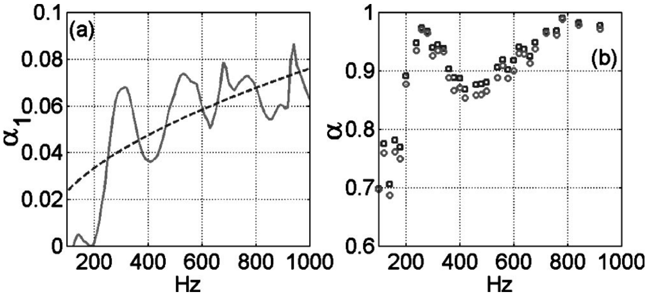

FIG. 4. The effect of sound energy dissipation along a rigid duct. (a) compares the measured energy dissipation coefficient of the straight duct segment in the present rig (———) with prediction of such losses based on a traveling wave theory (Pierce, 1991) (−−). (b) is the comparison of the absorption coefficient with (○) and without (□) correction for the sound energy loss along the rigid duct segments.

culated by the net sound energy flux into a control volume which encloses the long duct segment. As shown in Fig. 1, the control volume can be considered to be the duct segment from the center of microphones M3 and M4 to that of M1 and M2. Denote the intensity of sound traveling from the position of microphone *m* towards microphone *n* as I_{mn}, the total sound energy dissipated inside the control volume is found as $\delta I = I_{34} - I_{43} + I_{21} - I_{12}$, and an energy dissipation coefficient is defined as $\alpha_1 = \delta I/\bar{I}$ where $\bar{I}$ is the average of the four intensity magnitudes. To find α_1, the rig shown in Fig. 1 was revised as follows. The test specimen on the left-hand side duct was removed, and a loudspeaker was installed on the left-hand side to serve as the sound source. By using two microphones on the left-hand side and another two on the right-hand side, all the wave components can be found, hence α_1. The vibrator-piston assembly was installed in the middle segment of the duct which had a length of 60 cm. When the middle segment of the duct was removed, the total duct length became 1.0 m between the centers of the two pairs of microphones. The energy dissipation coefficient is shown in Fig. 4(a) as the solid line. The energy dissipation in this case is expected to come mainly from the friction between sound and the duct walls, for which the analytical prediction (see Pierce, 1991, Eq. 10-5.8) for a single traveling wave is also shown in Fig. 4(a) as a dashed line. The two lines are close to each other in general, validating the general assumption for the dissipation mechanism. The wavy behavior of the measured dissipation coefficient probably accounts for the standing wave effect. Since such standing wave composition is not known *a priori* in the eventual one-microphone measurement, the analytical prediction of attenuation for a traveling wave is used as a correction factor for the decay of each traveling wave along the duct. The effect of this correction is shown in Fig. 4(b), where the open squares are the results without the correction and open circles are those with attenuation correction. The mean correction is about 1.2% for α. Generally speaking, the correction is not large and such a correction can be further reduced or even ignored if the distance between the measurement microphone and the specimen is minimized. The current test rig had the provision for the two-microphone measurement for the validation purpose, and a reduction of duct length is anticipated when such provision is removed for practical use of the one-microphone method.

C. Piston response

The working principle of the present one-microphone method is based on the assumption that the radiated wave from the piston for a given voltage input, p_{rad}, is not affected by the location of the rigid end plate. Factors that uphold and undermine this assumption are briefly discussed here before a quantitative experimental examination of the assumption is reported. The actual amplitude of the piston vibration is influenced by the input mechanical impedance, say Z_{in}, derived from the fluid loading on the piston inside the duct (cf. Kinsler *et al.*, 2000). This impedance diverges at a duct resonance frequency when the measurement sample is a hard wall and all acoustic attenuations are ignored. Under this extreme condition, the constant p_{rad} assumption is unlikely to be upheld and the current method would fail around such resonance frequency. However, it is anticipated that the actual magnitude of Z_{in} is rather limited when the normal friction is accounted for. It is also limited by the finite dissipative element which normally exists in any specimen to be measured. The variation of Z_{in} at a nonresonant frequency is even more limited. Having said that, a loudspeaker made of paper cone is unlikely to possess sufficient mechanical impedance such that Z_{in} is deemed negligible. The device used in the current test is a B&K vibration exciter type 4809 with a force rating of 45 N. A piston of mass 294 g is attached as the payload. Note that a heavier piston would reduce the vibration amplitude but the system impedance can be further increased, leading to a better satisfaction of the constant p_{rad} assumption. The extent to which the piston vibration was affected by the swapping of the end plate position was investigated quantitatively. The response of the piston was measured by a B&K accelerometer (type 4374 with Nexus conditioning amplifier type 2692) placed on top of the piston. The voltage input to the vibrometer, v_{in}, and the acceleration output from the accelerometer, v_{out}, were sampled simultaneously by the computer. The amplitude ratio of the two signals is shown in Fig. 5 for the range of frequencies from 60 to 1000 Hz. The solid line is the result for the first position of the end plate, $L_a = 615$ mm, and open circles for the second, $L_b = L_a + 40$ mm. The two results are hardly distinguishable in the figure. The average deviation is 0.8%, and the effect of such deviation on the results of one-microphone measurement is found to be negligible.

D. Inaccuracy caused by the calibration error

Whether the deviation between the one- and two-microphone measurements is large or not can be judged by the range of uncertainty involved in the latter method due to microphone calibration. Assuming that the transfer function between the actual sound pressure *p* and the digital reading *A* from a microphone input channel is J_1, J_2 for the two microphones, respectively, and that a standing wave pattern is formed by an incident wave Ie^{-ikx} and a reflected wave Re^{ikx}, where $x=0$ is located at the center of the two micro-

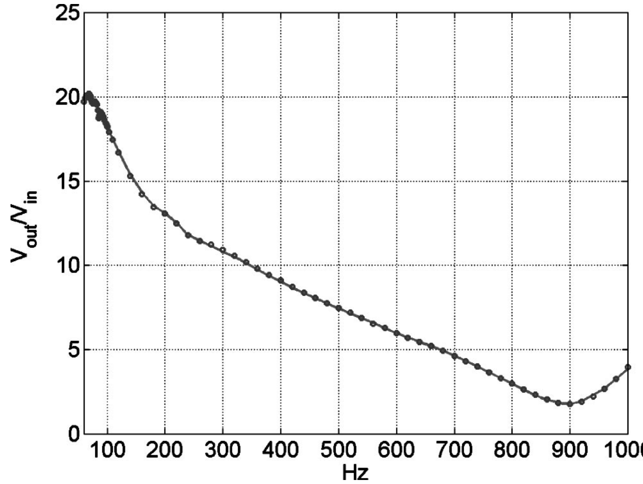

FIG. 5. Comparison of the amplitude ratio of signals from the piston acceleration and the voltage input to the vibrator when the end plate is located at $L_a = 615$ mm (———) and $L_b = L_a + 40$ mm (○).

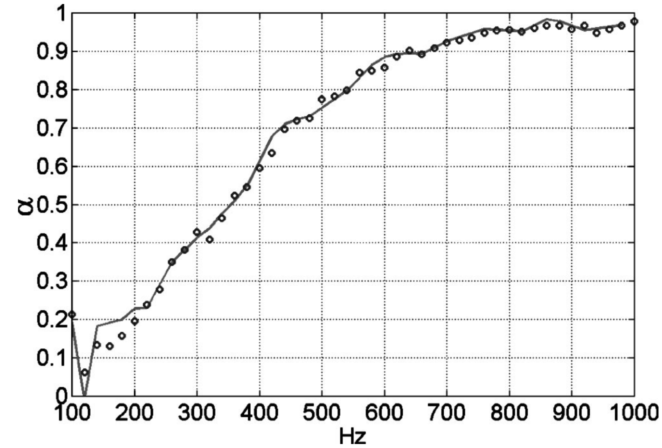

FIG. 7. The absorption coefficient measured by an electret microphone in the present rig (○) compared with the two-microphone measurement using two B&K microphones (———).

phones separated by a distance of s, the wave components I and R are resolved in one session of two-microphone measurement as follows:

$$I = \frac{J_1 A_1 e^{-ik(L_1+s)} - J_2 A_2 e^{-ikL_1}}{e^{-iks} - e^{iks}} \quad \text{and}$$

$$R = \frac{-J_1 A_1 e^{ik(L_1+s)} + A_2 J_2 e^{ikL_1}}{e^{-iks} - e^{iks}}.$$

The linear reflection coefficient R/I is

$$\frac{R}{I} = e^{2ikL_1}\left(\frac{-A_1 e^{iks} + A_2 J}{A_1 e^{-iks} - J A_2}\right), \tag{9}$$

where $J = J_2/J_1$ is the complex ratio of the microphone responses. When the complex ratio J is subject to an uncertainty of δJ, the resultant energy coefficients of reflection and absorption can be found out easily. Figures 6(a) and (b) show the amplitude and phase of calibration factor J, respectively. Two typical sets of data are shown for two calibration exercises, and the difference between the two gives an estimate for the magnitude ratio $|\delta J|$ and phase angle difference $\delta\theta$. Typically, the difference in amplitude was about 0.002 for frequencies greater than 300 Hz. However, much higher deviation was found at lower frequencies. The effect of δJ on the measured absorption coefficient α for the 60-mm-deep fiberglass filling in the present rig is shown in Figs. 6(c) and (d). Figure 6(c) shows the maximum (dashed line) and minimum (solid line) level of the absorption coefficient when $|J|$ changes from 0.99 to 1.01 and phase angle θ changes from -0.005 to 0.015. Figure 6(d) shows the range of absorption coefficient $\delta\alpha$. It is found that $\delta\alpha$ associated with such δJ can be greater than the deviation between the one-microphone and two-microphone measurements as shown in Fig. 2. The uncertainty is also larger than the frictional losses shown in Fig. 4(a). The comparison between the two-microphone method and Chu's (1986b) one-microphone method shows that the deviation for the reflection coefficients at very low frequencies (<250 Hz) is about 0.1, which is slightly poorer than what is achieved here (cf. Fig. 3 of Chu, 1986b).

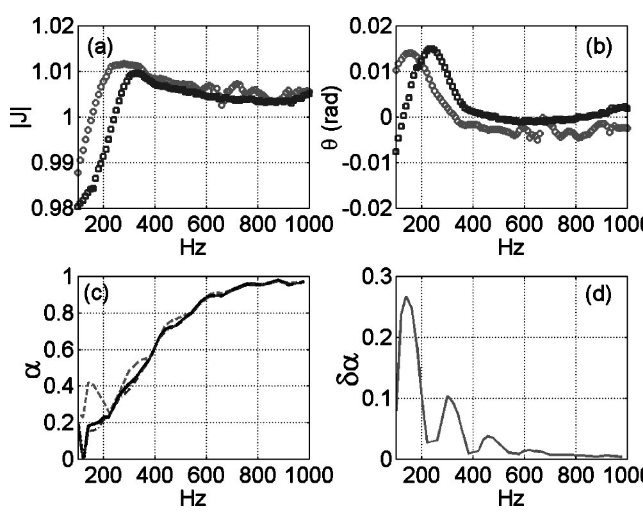

FIG. 6. The uncertainty of the two-microphone method. (a) shows the magnitude of the calibration factor J, and (b) is the phase of J during two calibration trials (□,○). (c) is the maximum (−−) and minimum level (———) of absorption coefficient caused by the variation of J. (d) is the uncertainty of the absorption coefficient caused by such variation.

E. Use of an electret microphone

The accuracy of the one-microphone measurement depends on the consistency of the transfer function between the measurement microphone and the sound source, and it eliminates the need of calibration between two microphones. To demonstrate the full advantage of this method, a very low-budget microphone was used instead of B&K's $\frac{1}{2}$-in. condenser-type microphones which have a flat frequency response down to at least 20 Hz. A miniature (0.1-in.) electret microphone produced by Tibbetts Industries (151 series) was tested. It had a flat frequency response from 300 to 3000 Hz, and its response at 100 Hz was 4 dB below that at 300 Hz. Figure 7 shows the comparison of α measured by using such an electret microphone in the present method with that of the two-microphone method. The medium deviation was about 1.9%, slightly higher than 1.4% from B&K microphones.

V. CONCLUSIONS

A new rig of one-microphone measurement method for in-duct standing waves is proposed and experimentally validated against the well-established two-microphone method. The new rig involves the use of a side-branch sound source and a movable rigid plate which provides the necessary configuration variation to achieve two independent measurements. The main advantage of the rig is that the measurement microphone is installed at its fixed position during the measurements. Results are summarized as follows.

(1) The use of a fixed microphone eliminates the need to drill many microphone insertion holes as required by the two-microphone method and the existing one-microphone method.
(2) The agreement of the sound reflection and absorption coefficients between the present one-microphone method and the two-microphone method is very satisfactory.
(3) The complete flexibility for the rigid plate to vary its position eliminates the blind spots in spectrum where measurements are rendered impossible when the separation distance between the two microphone positions coincides with the half wavelength.
(4) Sound energy losses and other factors of uncertainties are discussed, and the errors are found to be generally acceptable when compared with the uncertainties in the two-microphone measurement arising from the microphone calibration.
(5) A very low budget electret microphone is also found to yield satisfactory results in the present one-microphone method.

ACKNOWLEDGMENTS

The authors thank the Research Grants Council of the Hong Kong SAR Government for its support of the project (PolyU 5169/02E). Very careful checking by an anonymous reviewer also improved the manuscript.

Bodén, H., and Åborn, M. (**1986**). ''Influence of errors on the two-microphone method for measuring acoustic properties in ducts,'' J. Acoust. Soc. Am. **79**, 541–549.
Chu, W. T. (**1986a**). ''Extension of the two-microphone transfer function method for impedance tube measurement,'' J. Acoust. Soc. Am. **80**, 347–348.
Chu, W. T. (**1986b**). ''Transfer function technique for impedance and absorption measurements in an impedance tube using a single microphone,'' J. Acoust. Soc. Am. **80**, 555–560.
Chu, W. T. (**1988**). ''Further experimental studies on the transfer-function technique for impedance tube measurements,'' J. Acoust. Soc. Am. **83**, 2255–2260.
Chung, J. Y., and Blaser, D. A. (**1980a**). ''Transfer function method of measuring in-duct acoustic properties. I. Theory,'' J. Acoust. Soc. Am. **68**, 907–913.
Chung, J. Y., and Blaser, D. A. (**1980b**). ''Transfer function method of measuring in-duct acoustic properties. II. Experiment,'' J. Acoust. Soc. Am. **68**, 914–921.
Fahy, F. J. (**1984**). ''Rapid method for the measurement of sample acoustic impedance in a standing wave tube,'' J. Sound Vib. **97**, 168–170.
ISO10534-2:1998(E) (**1998**). Acoustic-Determination of sound absorption coefficient and impedance in impedance tubes (International Standard Organization).
Jones, M. G., and Parrott, T. L. (**1989**). ''Evaluation of a multi-point for determining acoustic impedance,'' Mech. Syst. Signal Process. **3**, 15–35.
Kinsler, L. E., Frey, A. R., Coppens, A. B., and Sanders, J. V. (**2000**). *Fundamentals of Acoustics* (Wiley, New York).
Lippert, W. K. R. (**1953**). ''The practical representation of standing waves in an acoustic impedance tube,'' Acustica **3**, 153–160.
Pierce, A. D. (**1991**). *Acoustics: An Introduction to its Physical Principles and Applications* (Acoustical Society of America, New York).
Seybert, A. F., and Ross, D. F. (**1977**). ''Experimental determination of acoustic properties using a two-microphone random-excitation technique,'' J. Acoust. Soc. Am. **61**, 1362–1370.
Seybert, A. F., and Soenarko, B. (**1981**). ''Error analysis of spectral estimates with application to the measurement of acoustic parameters using ransom sound fields in ducts,'' J. Acoust. Soc. Am. **69**, 1190–1199.